Plasma Physics and Controlled Fusion

Crossmark

RECEIVED
dd Month yyyy

REVISED
dd Month yyyy

MANUSCRIPT PAPER: PLASMA PHYSICS AND CONTROLLED FUSION

Outcomes of activation measurements and analyses of ITER materials during JET DTE3 operations

L. W. Packer[1], P. Batistoni[3], S. C. Bradnam[1], M. Fabbri[4], N. Fonnesu[3], M. R. Gilbert[1], Z. Ghani[1], M. Gorley[1], C. L. Grove[1], A. Harte[1], L. Jones[1], R. Kierepko[4], E. Łaszyńska[5,6], I. Lengar[7], X. Litaudon[2,8], S. Loreti[3], J. W. Mietelski[4], M. I. Savva[9], C. R. Shand[1], I. E. Stamatelatos[9], A. N. Turner[1], T. Vasilopoulou[9], R. Villari[3], A. Wójcik-Gargula[4], J. Włodarczyk[5] and JET Contributors*

[1]United Kingdom Atomic Energy Authority, Culham Science Centre, Abingdon, Oxon, OX14 3DB, UK
[2]EUROfusion - Programme Management Unit, Culham Science Centre, OX14 3DB, Abingdon, UK
[3]ENEA - Department of Fusion and Technology for Nuclear Safety and Security, via E. Fermi 45, 00044 Frascati (Rome), Italy
[4]Institute of Nuclear Physics, Polish Academy of Sciences, PL-31-342 Krakow, Poland
[5]Institute of Plasma Physics and Laser Microfusion, 01-497 Warsaw, Poland
[6]AGH University of Krakow, Faculty of Energy and Fuels, Department of Nuclear Energy and Radiochemistry, 30-059 Krakow, Poland
[7]Reactor Physics Department, Jožef Stefan Institute, Jamova cesta 39, SI-1000 Ljubljana, Slovenia
[8]CEA, IRFM, F-13108 Saint-Paul-lez-Durance, France
[9]Institute of Nuclear and Radiological Sciences, Technology, Energy and Safety, NCSR Demokritos, Athens, 15310, Greece
*See the author list of "Overview of T and D-T results in JET with ITER-like wall" by C. F. Maggi et al. 2024 Nucl. Fusion 64 112012

E-mail: lee.packer@ukaea.uk

Keywords: neutronics, activation, DTE2, DTE3

Abstract

The 2023 JET deuterium-tritium (D–T) experimental campaign (DTE3) achieved record fusion energy output (69 MJ), providing a unique 14.1 MeV neutron environment for irradiation studies. A range of ITER material samples were exposed in a Long-Term Irradiation Station (LTIS) within the JET nuclear environment to neutron fluxes up to 2×10^{13} n/cm^2/s, reaching total fluences of 7×10^{15} n/cm^2—the highest achieved in a tokamak. Post-irradiation analysis using high-resolution gamma spectrometry across five laboratories identified a range of neutron-induced activation products present in these samples, which were quantitatively compared with neutronics simulation predictions. Complementary neutron fluence measurements with metallic dosimetry foils located in the LTIS enabled validation of the simulation approach via MCNP and FISPACT-II codes. The DTE3 results, combined with those from prior D–T campaigns, together provide a highly valuable dataset for ITER, supporting the validation of predictive modelling tools towards sustained high power D–T operations.

1 Introduction

The Joint European Torus (JET) has provided a unique facility for deuterium-tritium (D–T) plasma operations, generating essential learning and data from the nuclear environment of a tokamak. Building on the 2021 D–T campaign (DTE2) and prior activities through deuterium plasma operations, the 2023 DTE3 campaign [1] further extended the experimental and technological exploitation of JET, yielding new data for neutron transport and activation phenomena for materials. The EUROfusion programme, initiated under the JET3 project [2, 3, 4] and continued through the 'Preparation of ITER Operations' (PrIO) work-package [5, 6, 7] since 2020, has collected nuclear fusion-related data of high relevance to ITER.

D–T operations at JET have enabled a broad range of technology-focused experiments to advance nuclear technology, validate simulation codes, and refine methodologies for ITER. Recent activities, described in [6], include neutron activation measurements and analysis of ITER-relevant

materials, development of diagnostic techniques [8, 9, 10, 11, 12, 13, 14, 15], irradiation of functional materials for damage studies, neutron streaming and shutdown dose rate (SDDR) benchmarks, calibration of 14 MeV neutron diagnostics, TBM detector testing, evaluation of advanced shielding, and collection of occupational radiation exposure (ORE) and nuclear waste data, water activation in the JET cooling loop and neutron-induced Single Event Effects (SEE) studies on electronics.

During the JET DTE3 experimental campaign, 69 ITER-relevant material samples—including EUROFER 97, tungsten (W), CuCrZr, Al–bronze, Inconel 718, Alloy 660, XM-19 and 316L stainless steel—were irradiated in the Long-Term Irradiation Station (LTIS) to neutron fluxes up to 2×10^{13} n/cm^2/s and total fluences of 7×10^{15} n/cm^2, the highest achieved in a tokamak to date. Post-irradiation analysis using high-resolution gamma spectrometry across five laboratories (ENEA, IFJ PAN, IPPLM, NCSRD, and UKAEA) enabled quantification of neutron-induced activation products and identification of impurities or unexpected isotopes. Complementary neutron dosimetry diagnostics, using 20 high-purity metallic foils including Y, Co, Ni, and Fe, were used to measure the neutron fluence. These results are summarised within this paper and serve to extend validation datasets for MCNP and FISPACT-II simulations, further supporting predictive modelling of nuclear phenomena for ITER and other fusion machines.

The outcomes of the DTE3 campaign are of direct significance for ITER's nuclear phase and associated safety demonstrations, particularly in light of its revised schedule for nuclear operations [16]. This work presents comparisons between measured activation data, calculated inventories, and detailed JET neutronics models. Although obtained at lower fusion power and duration than is foreseen for ITER scenarios, these rare results from D–T tokamak operations do provide benchmark data to extrapolate to ITER conditions that can support operational readiness for sustained high-power D–T operation through validated neutronics tools.

2 Materials and sample preparation

A representative set of ITER-relevant materials, sourced by Fusion for Energy (F4E) from multiple ITER manufacturers, was selected to reflect different ITER components. The material identifiers are indicated in the C/E (calculation over experimental) plots shown in Figure 3. The corresponding reference material compositions are reported in [7].

Material samples were prepared into discs by UKAEA's Special Techniques Group using electrical discharge machining (EDM) which were uniquely etched using a punching method for identification. Some of the samples, including some CuCrZr and W samples, were polished to remove surface brass. Elemental composition certificates accompanying each batch, together with reference data from [17, 18], were used as inputs to the inventory simulation calculations described in section 4.

3 Sample retrieval and post-irradiation analysis

The Long-Term Irradiation Station (LTIS) assembly containing ITER-relevant material samples was retrieved in 2024 following a period of radiological cooling after the final DTE3 neutron exposure in December 2023. Handling and disassembly operations were conducted at UKAEA under controlled conditions. Lessons from previous operations informed minor design adjustments for disassembly of the LTIS, such as replacing stainless steel screws with aluminium-bronze-coated variants to facilitate easier retrieval of samples.

The samples were distributed to European laboratories in 2025 (ENEA, IFJ PAN, IPPLM, NCSRD) for post-irradiation analysis. Each laboratory measured sample mass, identified radionuclides, determined decay-corrected activity, and evaluated associated uncertainties. High-resolution gamma spectrometry systems—including detectors with Compton suppression capabilities—were calibrated using radionuclide sources and/or LabSOCS-generated efficiency curves traceable to primary standards.

3.1 Gamma spectrometry analysis

All participating laboratories applied high-resolution gamma spectrometry to acquire emission spectra. Detector calibration, energy verification, and efficiency determination followed established methodologies [4, 7], enabling inter-laboratory comparison and reliable activity quantification. The use of Compton suppression systems by some laboratories has enhanced signal-to-background ratios for some radionuclides, improving the detection of low-yield or overlapping gamma lines.

Isotopic analysis across 69 irradiated samples enabled identification of 16 principal activation products. An example spectra from a CuCrZr sample demonstrate resolution of characteristic lines associated with radionuclide gamma emissions, with and without Compton suppression, is shown in Figure 1. Example details of the analysis methodology applied by UKAEA is covered in [19].

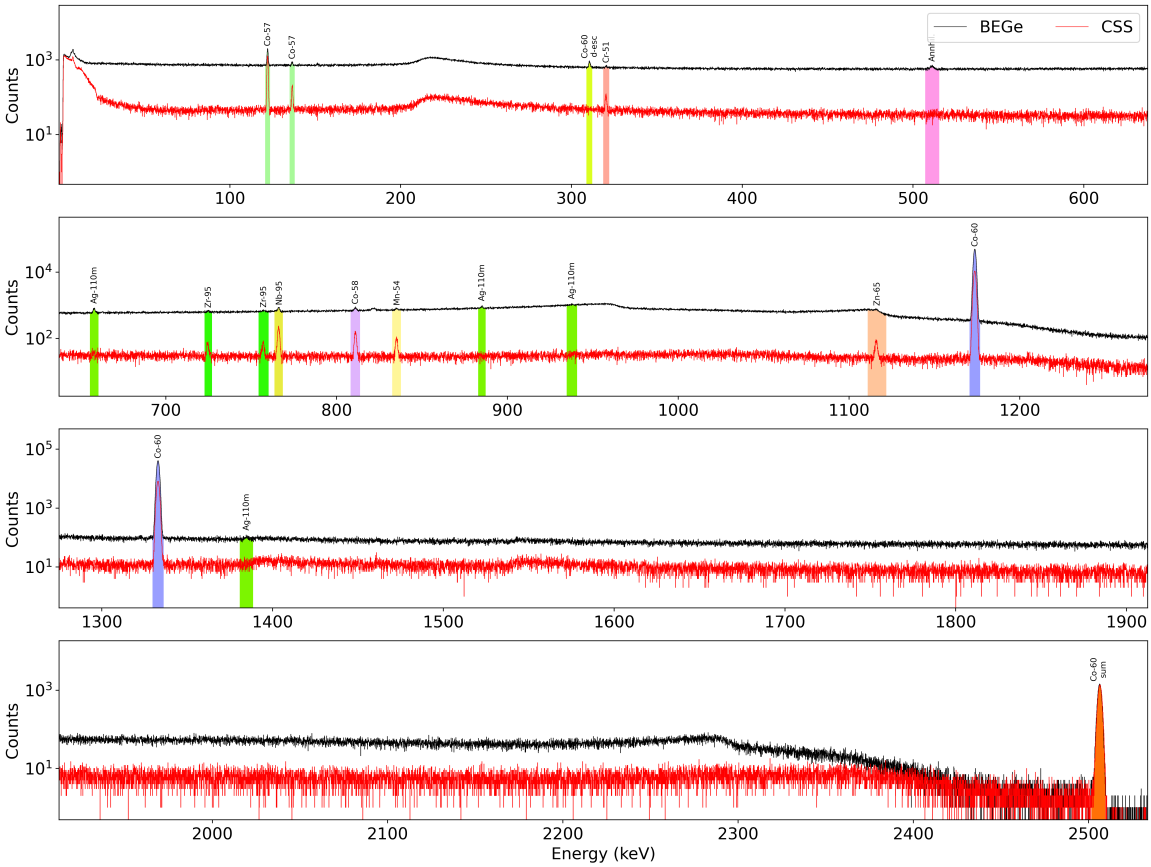

Figure 1. Gamma spectrum measurement from a CuCrZr sample (position ID: 15_4). Black and red lines correspond to data acquired using the BEGe detector with and without the Compton suppression system (CSS).

4 Simulation methodology for radionuclide activity predictions

Neutron transport and activation simulations were performed for all samples located within the LTIS to predict the time-dependent evolution of nuclides during irradiation and subsequent decay. The methodology adopted followed the approach taken for previous JET campaigns, detailed in [7]. A detailed MCNP model [20] of JET was used which included geometric representations of the LTIS sample loading configuration that was deployed during DTE3. Neutron spectra, fluxes and relevant reaction rates for D–D, and D–T plasma components were calculated for each sample location.

These neutron spectra were input to FISPACT-II [21] for inventory calculations, incorporating experimental neutron yield data and time-dependent irradiation profiles. Self-shielding effects were addressed using spectrum-averaged cross sections from IRDFF-II [22], and with JEFF 3.3 and TENDL-2017 libraries applied for reactions that were not present within the IRDFF-II library. Daily irradiation pulses were computed by combining measured neutron yields with MCNP flux normalization at the sample positions. Activities were calculated separately for each neutron component and summed to yield total nuclide inventories.

For DTE3, the LTIS was installed on [*8th February 2023*] with first exposure on 27th February (shot no.101990), and retrieved on 14th June 2024 after a total of 2925 experimental shots with a neutron yield of 7.88 $\times 10^{20}$. Neutron yields from the D–T, T–T, and D–D components were measured using the KN1 fission chamber system [23, 24] and used to model the temporal evolution of neutron fluence. The bottom panel of Figure 2 illustrates the predicted daily neutron fluence for each component and the corresponding calculated specific activities for a CuCrZr sample (reference 15_4, measured by UKAEA). Inset plot show the per-unit lethargy neutron spectra averaged over the sample volume for D–D and D–T spectrum components.

5 Results: Measurements and comparison of C/E Ratios

Calculated-to-experimental (C/E) ratios derived from the DTE3 and related experiments are presented in this section. Figure 3(a) and (b) show all individual C/E values, grouped by measured isotope and by material type, respectively. The corresponding weighted-average C/E results by material type are shown in Figure 3(c).

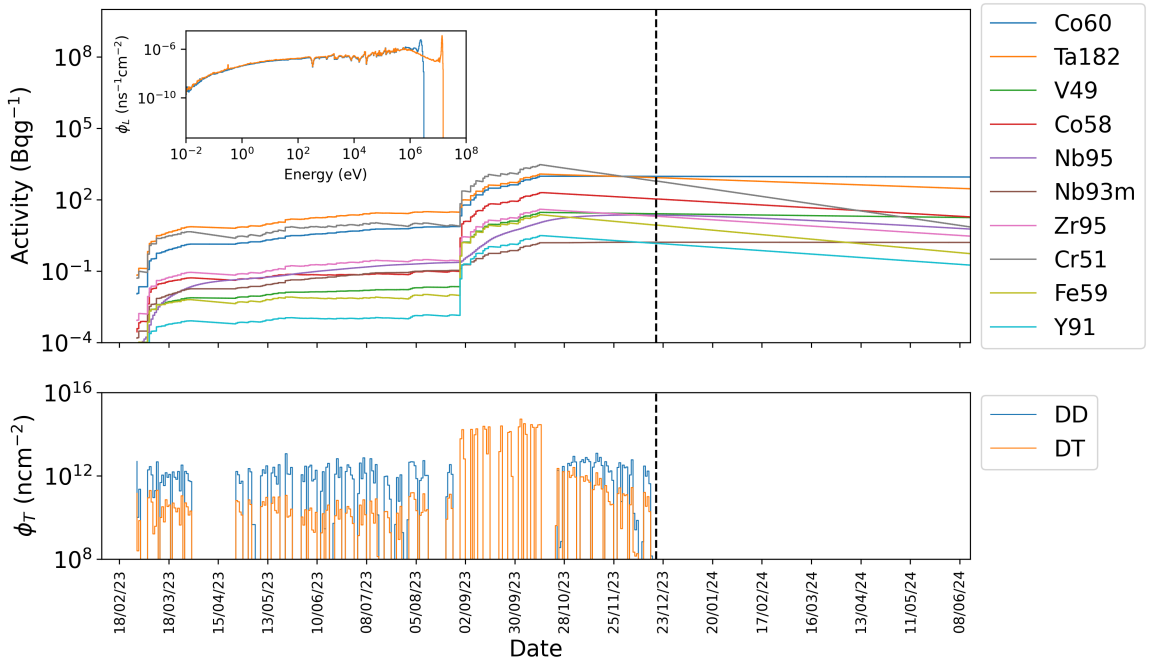

Figure 2. Predicted temporal evolution of dominant radionuclide activities during and after JET irradiation of a CuCrZr sample (15_4). The black dashed line marks the final JET operation on 18th December 2023 and the last day the LTIS saw JET neutrons, following its installation on 8th February 2023. The date extends to when the LTIS was retrieved from JET on 14th June 2024. Inset plot show the neutron per unit lethargy, ϕ_L, averaged over the sample volume within the LTIS, calculated using MCNP. Bottom: daily neutron fluence ϕ_T averaged over the LTIS sample volume for D–D, D–T, and T–T components.

Overall, Figure 3 demonstrates good agreement between calculations and measurements for the majority of isotopes. An exception is ^{65}Zn, which is discussed in detail in [7]. Notwithstanding this general agreement, several notable discrepancies are observed for CuCrZr, EUROFER, and W, which are briefly highlighted here.

For CuCrZr, very low weighted average (weighted by the inverse variance) C/E values were obtained for ^{54}Mn and ^{57}Co, with values below 5.84×10^{-9}. and a high C/E value of 10.5 was observed for ^{58}Co. Relevant to CuCrZr is the Wójcik-Gargula et al. [25] analysis, who report the presence of trace silver impurities in irradiated CuCrZr alloys and quantify their radiological impact, particularly Ag-110m and through predictions Ag-108m, further highlighting the importance of minor elements in activation assessments for ITER-relevant materials.

In the case of EUROFER, ^{60}Co is significantly overestimated, with a C/E value of 5.6. For W, low C/E values are observed for ^{54}Mn and ^{60}Co, with values of 0.04 and 0.11, respectively, while a high C/E value of 11.7 is again observed for ^{58}Co.

Results from dosimetry foil analysis are reported in [19], where good overall agreement is demonstrated, with a weighted-average C/E across all measured reactions of 0.97 ± 0.01. When considering threshold reactions only, the weighted-average C/E across all measured reactions is 0.91 ± 0.006. For capture reactions, however, the weighted-average C/E indicates a systematic overestimation, with a value of 1.53 ± 0.13.

6 Discussion and conclusions

The 2023 JET DTE3 campaign has provided a comprehensive experimental dataset for ITER-relevant materials exposed to high-energy D–T neutron irradiation. A total of 69 samples, including EUROFER 97, tungsten, CuCrZr, Inconel 718, and 316L stainless steel, were irradiated in the Long-Term Irradiation Station (LTIS), achieving neutron fluxes up to 2×10^{13} n cm^{-2} s^{-1} and total fluences of 7×10^{15} n cm^{-2}, the highest reported in a tokamak to date. Post-irradiation gamma spectrometry, conducted across five laboratories, enabled quantification of multiple radionuclides and identification of trace impurities. Combined with the previously reported DTE2 results [7], the DTE3 dataset represents the first systematic characterisation of a diverse array of ITER-relevant materials irradiated within a tokamak-based D–T neutron environment. Here, we present the dataset and an initial analysis comparing calculated and experimental results.

Dosimetry foil measurements in the LTIS show good agreement between calculated fast-neutron

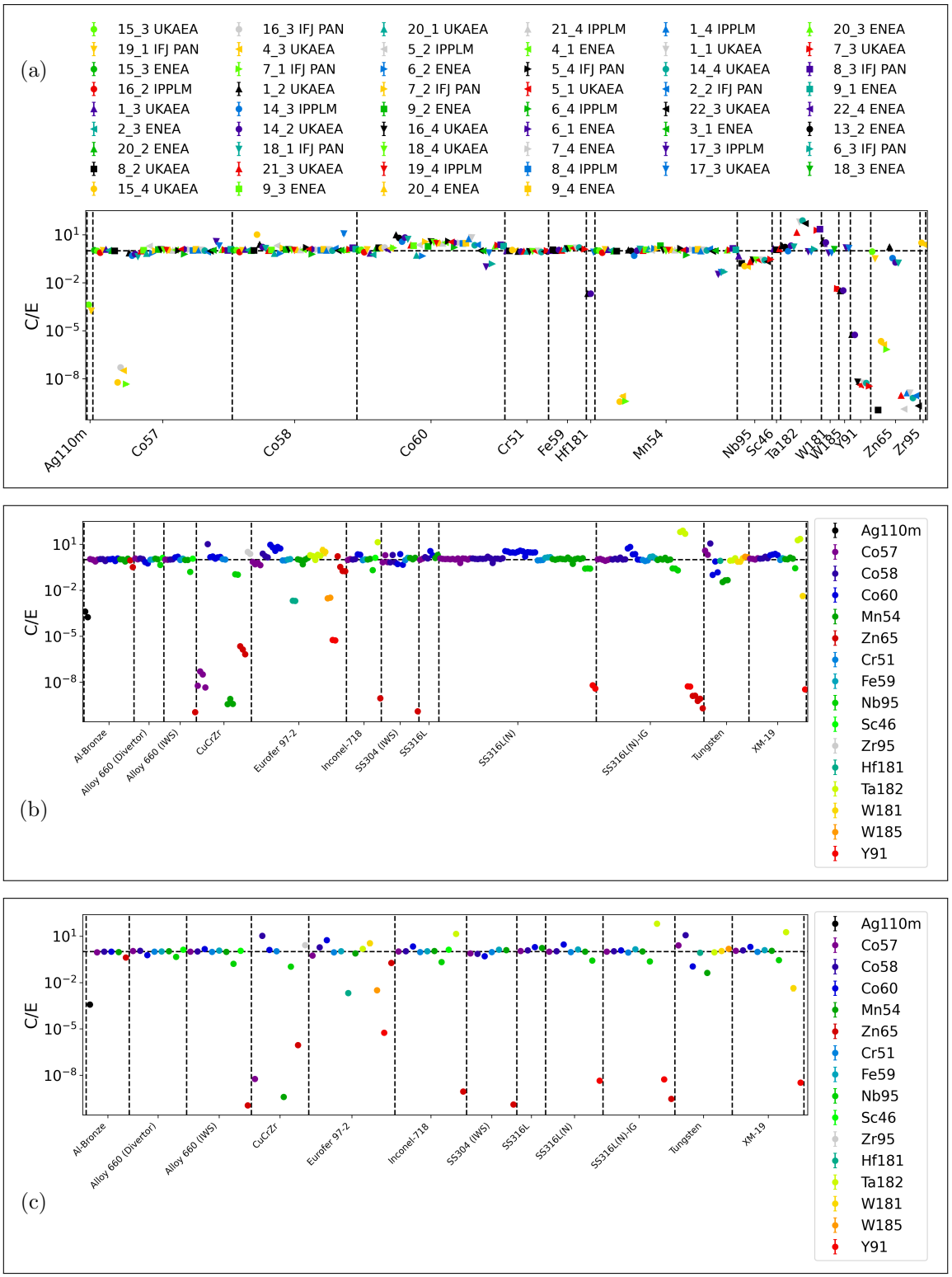

Figure 3. C/E values for measured and calculated ITER materials: (a) all results grouped by measured isotope. The legend indicates the LTIS position–depth–laboratory ID, as described in [7]; (b) all results grouped by material type; (c) weighted average results by material type.

fluence and experimental observations. The weighted-average calculated-to-experimental (C/E) ratio across all dosimetry measurements was 0.97 ± 0.10, confirming that the LTIS neutron environment is well characterised.

C/E comparisons for irradiated materials reveal material- and isotope-dependent behaviour. Several radionuclides, including ^{46}Sc, ^{51}Cr, ^{59}Fe, and ^{58}Co, exhibit good agreement with calculations, typically within 30%. In contrast, C/E discrepancies for some radionuclides present in irradiated CuCrZr, EUROFER, and W highlight the influence of trace elemental impurities not specified in material certificates, which significantly affects the production of certain radionuclides. Ongoing work includes independent elemental characterisation using mass spectrometry and the development of accelerator mass spectrometry (AMS) methods to detect long-lived, difficult-to-measure radionuclides such as ^{91}Nb, ^{94}Nb, and ^{93}Mo. These isotopes are relevant for assessing waste arisings and other post-irradiation analyses. Vivo-Vilches et al. [15] explore the potential of AMS to quantify these radionuclides in fusion-relevant materials, potentially providing a complementary ultra-sensitive technique to conventional gamma spectrometry.

Overall, the DTE3 results establish a robust validation dataset for fusion neutronics tools, supporting predictive modelling, design optimisation, and operational readiness for ITER's nuclear phase. They demonstrate that advanced neutronics codes, when coupled with high-quality nuclear data and well-characterised experimental inputs, can reliably predict nuclide inventories in materials exposed to D–T fusion neutron fields. This capability is essential for safety case development, shutdown dose rate assessments, and planning sustained high-power D–T operations in ITER and future fusion devices.

Acknowledgments

This work has been carried out within the framework of the EUROfusion Consortium, funded by the European Union via the Euratom Research and Training Programme (Grant Agreement No 101052200 — EUROfusion). Views and opinions expressed are however those of the author(s) only and do not necessarily reflect those of the European Union or the European Commission. Neither the European Union nor the European Commission can be held responsible for them.

This work has been part-funded by the EPSRC Fusion Grant 2022/27 [grant number EP/W006839/1]. To obtain further information on the data and models underlying this paper please contact PublicationsManager@ukaea.uk

References

[1] Maggi, C.F. et al, "Overview of T and D–T results in JET with ITER-like wall," *Nuclear Fusion*, vol. 64, p. 112012, aug 2024.

[2] L. Packer *et al.*, "Status of ITER material activation experiments at JET," *Fusion Engineering and Design*, vol. 124, 2017.

[3] L. Packer *et al.*, "Activation of ITER materials in JET: nuclear characterisation experiments for the long-term irradiation station," *Nuclear Fusion*, vol. 58, no. 11, p. 116001, 2018.

[4] L. W. Packer *et al.*, "Technological exploitation of the JET neutron environment: progress in ITER materials irradiation and nuclear analysis," *Nuclear Fusion*, vol. 61, 2021.

[5] X. Litaudon et al., "EUROfusion contributions to ITER Nuclear Operation," *IAEA FEC Proc.*, 2023.

[6] R. Villari *et al.*, "Overview of deuterium-tritium nuclear operations at JET," *Fusion Engineering and Design*, vol. 179, p. 113129, 2025.

[7] Packer, L.W. et al., "ITER materials irradiation within the D–T neutron environment at JET: post-irradiation radioactivity analysis following the DTE2 experimental campaign," *Nuclear Fusion*, vol. 64, p. 106059, sep 2024.

[8] M. Savva *et al.*, "Application of VERDI detectors for neutron fluence measurements in real fusion environments," *Fusion Engineering and Design*, vol. 164, p. 112203, 2021.

[9] T. Vasilopoulou *et al.*, "Improved neutron activation dosimetry for fusion," *Fusion Engineering and Design*, vol. 146, pp. 1078–1081, 2019.

[10] A. Wójcik-Gargula *et al.*, "Studies on the behaviour of titanium activation foils during long-term exposure at the JET tokamak," *Fusion Engineering and Design*, vol. 177, p. 113056, 2022.

[11] I. Lengar *et al.*, "Characterization of JET neutron field in irradiation locations," *Fusion Engineering and Design*, vol. 146, pp. 1074–1077, 2019.

[12] N. Fonnesu *et al.*, "ITER-relevant experimental neutronic activities at JET during DTE3 and at the Frascati neutron generator," *Fusion Engineering and Design*, vol. 219, p. 115297, 2025.

[13] G. Stankunas, A. Tidikas, P. Batistoni, and I. Lengar, "Analysis of activation and damage of ITER material samples expected from DD/DT campaign at JET," *Fusion Engineering and Design*, vol. 125, 2017.

[14] A. Zohar *et al.*, "Long Term Neutron Activation in JET DD Operation," *EPJ Web Conf.*, vol. 253, p. 03005, 2021.

[15] C. Vivo-Vilches, E. Hrnjic, M. Martschini, L. W. Packer, K. Hain, and R. Golser, "Towards AMS measurements of ^{91}Nb, ^{94}Nb and ^{93}Mo produced in fusion environment," *Nuclear Instruments and Methods in Physics Research Section B: Beam Interactions with Materials and Atoms*, vol. 568, p. 165847, 2025.

[16] P. Barabaschi, A. Fossen, A. Loarte, A. Becoulet, and L. Coblentz, "ITER progresses into new baseline," *Fusion Engineering and Design*, vol. 215, p. 114990, 2025.

[17] M. R. Gilbert, J.-C. Sublet, and A. Turner, "Handbook of activation, transmutation, and radiation damage properties of the elements and of ITER materials simulated using FISPACT-II & TENDL-2015; ITER FW armour focus," tech. rep., CCFE-R(16)37, 2016.

[18] V. Barabash, "Chemical compositions of materials representing the components included into basic model for nuclear analysis of ITER," *IO, ITER-D-HTN8X3 V2.1*, vol. 1, 2016.

[19] C. Grove et al., "Improvements in gamma-ray spectroscopy techniques for characterising neutron-induced activation of ITER materials following DT irradiation," *Manuscript submitted to Plasma Physics and Controlled Fusion*, vol. xxx, p. xxx, 2025.

[20] J. C. Werner *et al.*, "MCNP Version 6.2 Release Notes," 2 2018.

[21] J.-C. Sublet, J. Eastwood, J. Morgan, M. Gilbert, M. Fleming, and W. Arter, "FISPACT-II: An Advanced Simulation System for Activation, Transmutation and Material Modelling," *Nuclear Data Sheets*, vol. 139, no. Supplement C, pp. 77 – 137, 2017. Special Issue on Nuclear Reaction Data.

[22] A. Trkov *et al.*, "IRDFF-II: A New Neutron Metrology Library," *Nuclear Data Sheets*, vol. 163, pp. 1–108, 2020.

[23] L. W. Packer *et al.*, "Activation of ITER materials in JET: nuclear characterisation experiments for the long-term irradiation station," *Nuclear Fusion*, vol. 58, no. 9, p. 096013, 2018.

[24] L. Packer *et al.*, "Neutron detection and measurement challenges at JET and ITER," in *Modern Neutron Detection* (I. Swainson, ed.), IAEA-TECDOC-1935, pp. 313–335, Vienna: INTERNATIONAL ATOMIC ENERGY AGENCY, 2020.

[25] A. Wójcik-Gargula *et al.*, "Evidence of silver impurities in irradiated Cu-based alloys and implications for the long-lived radioactive waste from ITER," *Fusion Engineering and Design*, vol. 224, p. 115575, 2026.